

Reconnaissance Report on the 31 March 2002 Earthquake on the East Coast of Taiwan

C. H. Loh,^{a)} M.EERI, K. C. Tsai,^{a)} M.EERI, L. L. Chung,^{b)} and C. H. Yeh^{b)}

On 31 March 2002, an earthquake of magnitude $M_L=6.8$ occurred in northeastern Taiwan that caused five deaths and damage to more than 300 buildings. The earthquake left some important lessons; these lessons were not considered after the 1999 Chi-Chi (Taiwan) earthquake but must be taken into account for the management of a similar situation in the future. This article first presents the strong motion characteristics found from the ground accelerations recorded from this event. In particular, the basin effects on the distribution of ground motion intensities observed in Taipei Basin are critically reviewed. Observations of some severe building damage following the earthquakes are then summarized. The building damage modes for this event, particularly due to the basin effect, are explored in detail. The characteristics of the building disaster reflected a typical situation that can occur in cities located in high seismic risk. Finally, the collapse of the two tower cranes on, and its impact on, the Taipei Financial Center construction site are described in detail. This article presents the main lessons learned from this earthquake in the light of work performed by the research team for natural disaster from the National Center for Research on Earthquake Engineering, Taiwan.

[DOI: 10.1193/1.1598438]

INTRODUCTION

Seismic disasters in Taiwan over the last twenty years, particularly the 1999 Chi-Chi earthquake, have caused a significant number of victims and direct physical damages. The National Science and Technology Program for Hazard Mitigation (NAPHM) and the National Center for Research on Earthquake Engineering (NCREE) have proven to be important organizations for seismic hazard mitigation (Loh et al. 2001). After the 21 September 1999 Chi-Chi earthquake there are still many technical, social, and economical aspects remaining to be considered in rehabilitation of cities and communities. Unfortunately, on 31 March 2002 at 2:52 p.m. local time, an earthquake of magnitude $M_L=6.8$ took place in the northeastern sea of Taiwan. The epicenter was located at 122.17°E and 24.24°N , about 44 kilometers away from the coastline of I-Lan County.

The focal depth was 9.6 kilometers. In about 96 seconds after the occurrence of earthquake, the Central Weather Bureau had calculated the epicenter, focal depth, earth-

^{a)} Dept. of Civil Engineering, National Taiwan University, Taiwan; and National Center for Research on Earthquake Engineering, Taiwan

^{b)} National Center for Research on Earthquake Engineering, 200, Section 3, Hsinhai Road, Taipei, Taiwan

Table 1. Ground motion intensity levels used in Taiwan

Level	Range of PGA (cm/sec ²)
I	0.8~2.5
II	2.5~8
III	8~25
IV	25~80
V	80~250
VI	250~400
VII	>400

quake magnitude, and intensities at various districts of Taiwan. Reports indicated several school buildings and office buildings were severely damaged in Taipei Basin. The ground motion intensity used in Taiwan is defined and listed in Table 1. The intensity at Nan-Ou, which is closest to the epicenter of the earthquake, was six according to the rapid earthquake information release system. In northern Taiwan, the intensity in most areas was larger than or equal to four. Even far away from the epicenter of the earthquake (about 100 to 120 kilometers away), the ground motion intensity in the Taipei metropolitan area was five, due to the basin effect.

More than 1,800 aftershocks occurred between 31 March and 19 April 2002. Figure 1 shows the epicenter of the earthquake and a number of major aftershocks. Most of the aftershocks occurred within six days after the main shock. The largest aftershock occurred on 4 April at the northwest of the main shock, with a focal depth of 10.3 kilometers and magnitude $M_L=5.4$. These aftershocks did not cause further damage. It is also noted that the distribution of aftershocks is concentrated in a small region to the northwest of the epicenter of the main shock. The phenomenon is consistent with the tectonics in that region, i.e., the Philippine Sea Plate subducts beneath the Eurasian Plate to the north along Ryukyu Trench. This paper presents general observations following the 31 March 2002 earthquake, which has been the second largest seismic disaster in the past 15 years in Taiwan. This article is a reconnaissance-type of report based on the observations of some topics discussed below.

GROUND MOTION CHARACTERISTICS OF 31 MARCH EARTHQUAKE

FREE-FIELD GROUND MOTION

Based on the free-field strong-motion data collected by the Seismology Center of the Central Weather Bureau (CWB), the scenario peak ground acceleration (PGA) distribution around the island is calculated using HAZ-Taiwan earthquake assessment methodology (Loh and Yeh 1998) and shown in Figure 2. The maximum PGA occurred in the northeastern region (I-Lan County) of Taiwan.

Figure 3 shows the attenuation of intensity of the 31 March earthquake in terms of PGA and spectral acceleration (5% damping) values, i.e., $S_a(T=0.3)$ and $S_a(T=1.0)$. The

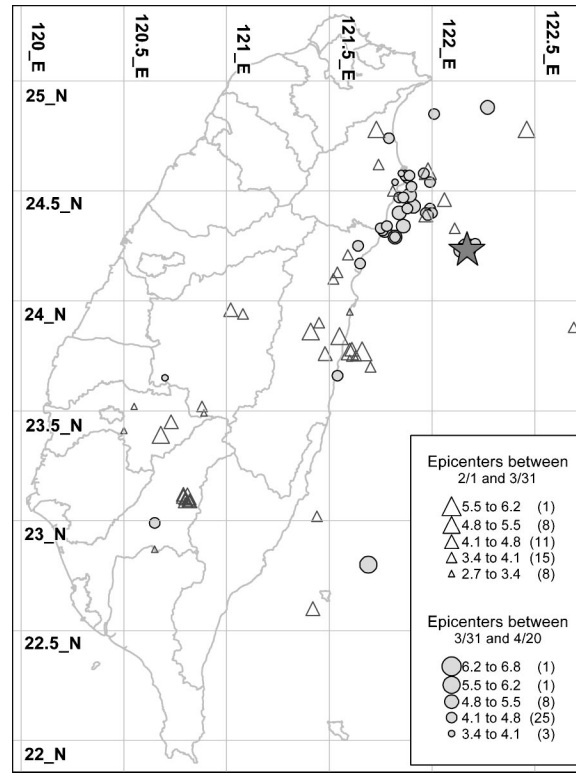


Figure 1. Epicenter of the 31 March 2002 earthquake (marked by a star) and the distribution of epicenters of aftershock with magnitude greater than 3. The epicenters of aftershocks that occurred between 1 February and 20 April 2002 are also shown.

empirical attenuation forms of PGA, $S_a(T=0.3)$, and $S_a(T=1.0)$ are also plotted for comparison. The empirical attenuation forms shown as solid lines in Figure 3 was expressed as (Jean 2001)

$$S_D = A_0 e^{aM} [R + b e^{cM}]^{-d} \quad (1)$$

where S_D is the seismic demand; M and R are the earthquake magnitude and the site-to-source distance, respectively; and A_0 , a , b , c , and d are constants as shown in Table 2. Figure 3 shows good agreement between the collected data and the empirical attenuation forms except those in the Taipei area (as indicated in the figure). The peak ground accelerations in the Taipei area (at a distance of about 110 km from the epicenter) are generally larger than the average values of the empirical attenuation forms because of the basin effect, which will be explained later. The recorded spectral accelerations, shown in Figures 3b and 3c, are generally larger than the empirical attenuation forms, especially for those of $S_a(T=1.0)$. Thus, it seems to suggest that the ground motion induced by the 31 March earthquake contains larger low-frequency energy than expected.

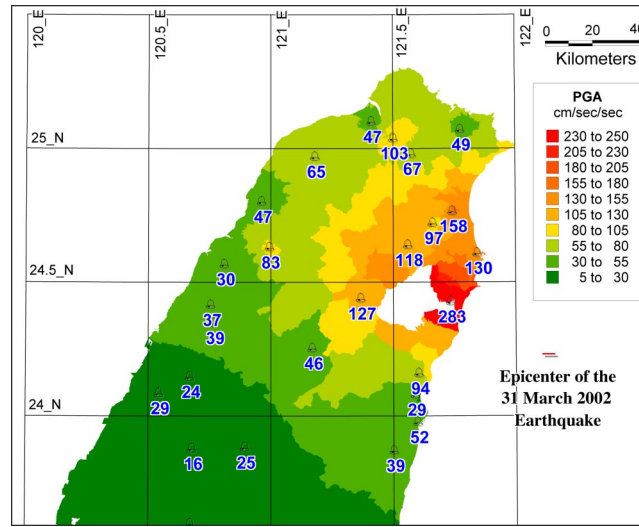


Figure 2. Based on the CWB real-time acceleration record, the distribution of PGA is calculated and interpolated for the 31 March 2002 earthquake.

In order to investigate the basin effects on ground intensity more thoroughly, the ground motion intensities in terms of PGA, PGV, $S_a(T=0.3)$, and $S_a(T=1.0)$ are calculated from several CWB strong-motion stations in and around Taipei Basin. The distribution of the selected CWB strong-motion stations is shown in Figure 4, and the calculated results are listed in Table 3. The PGA value is listed in accordance with the sorted epicentral distances. Although HWA045 is the closest station to the epicenter in Table 3, the ground motion parameters of station HWA045 are not the largest ones. The recorded acceleration time histories and the acceleration response spectra at station ILA050 are shown in Figure 5. The PGA along the east-west direction at ILA050 was about 283 cm/sec^2 , and the dominant frequency content of acceleration response spectra of station ILA050 was in between 2 and 10 Hz.

The ground motion recorded at station TAP085, which is located at the nearby outcrop mountain area of Taipei Basin, had low ground-motion intensities due to attenuation effect. The acceleration response spectra at TAP085 are shown in Figure 6 for comparison. However, in the vicinity of Taipei Basin, such as TAP035 and TAP053, the ground motion intensities start to increase significantly, and the peaks of acceleration response spectra remain in high-frequency range only, as shown in Figure 7. Other response spectra at the stations, such as TAP022 and TAP032, in the southeast side of Taipei Basin and with deeper soil deposit of alluvium layer show significant low-frequency content, as shown in Figure 8. At the location of station TAP022 the dominant frequency of the ground is about 1.2 sec. Based on the study of the distribution of dominant period of soil deposit in Taipei Basin, as shown in Figure 9 (Loh et al. 1998), two locations with longer vibration period are identified that were close to station TAP022 and TAP017. For this event, the most severe ground-shaking region is located in the

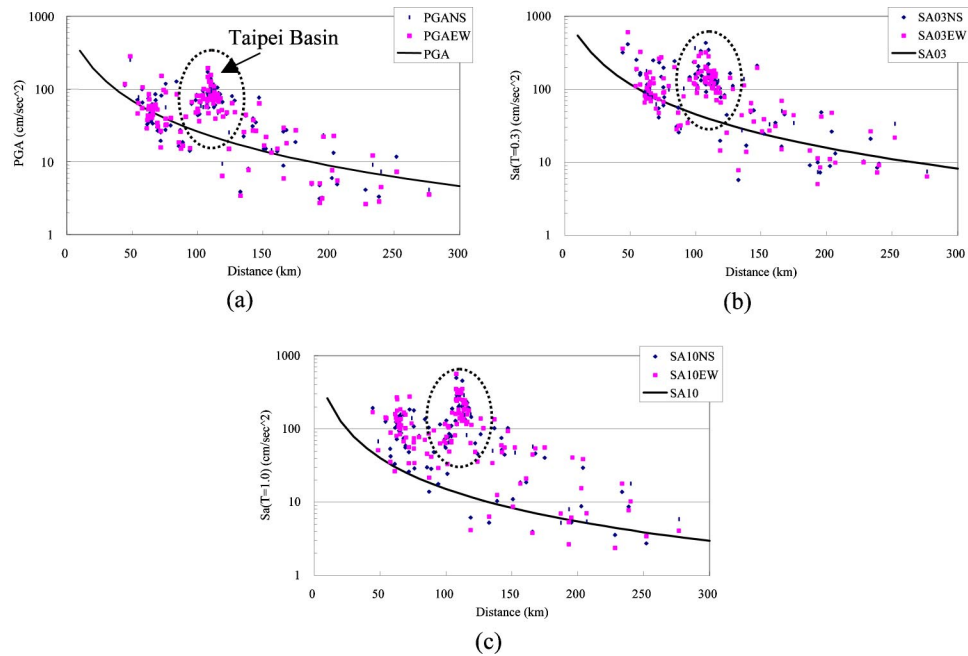


Figure 3. (a) PGA, (b) $S_d(T=0.3)$, (c) $S_d(T=1.0)$, in both east-west and north-south directions from recorded ground motion data during the 31 March 2002 earthquake. The attenuation forms in Equation 1 are also shown for comparison.

neighborhood of TAP022. This observation of period distribution of ground vibration from each recorded ground motion data in Taipei Basin is consistent with the identified distribution of dominant period of Taipei Basin.

STRUCTURAL RESPONSE

Besides the free-field strong-motion instrumentation, the Central Weather Bureau also had installed about 56 structural strong-motion array systems in buildings and bridges around Taiwan. Figure 10 shows the locations of the installed structural array systems in the Taipei area. For comparison, the locations of selected free-field stations were also shown in the same figure. Soon after the 31 March earthquake, the National Center for Research on Earthquake Engineering had collected the structural response

Table 2. Coefficients of the attenuation forms in Equation 1

Period	A_0	a	b	c	d
$S_d(T=0.3)$	0.04816	1.20645	0.15521	0.69900	1.72714
$S_d(T=1.0)$	0.0021184	1.35440	0.11479	0.60215	1.54714
PGA	0.02938	1.19950	0.14667	0.69689	1.73413

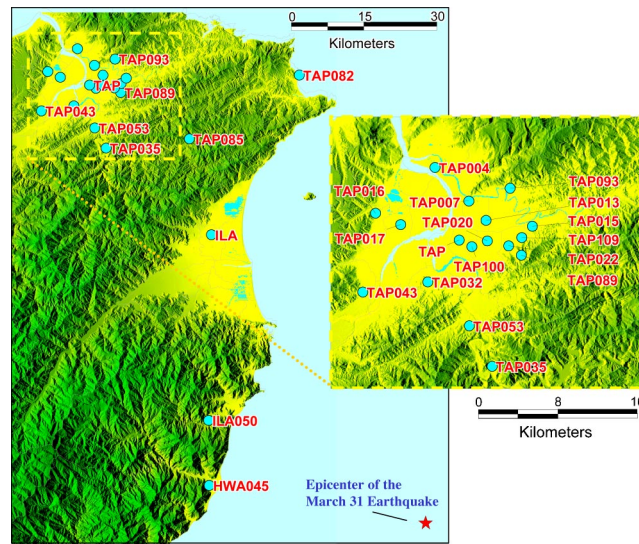


Figure 4. Distribution of the CWB strong-motion stations, which were selected to calculate ground motion parameters, as listed in Table 3.

data from the Taipei area. The data were available and were analyzed immediately after the earthquake. As examples, Figures 11 and 12 show the acceleration time histories and Fourier amplitude spectra, respectively, at the basement and the roof of building TAPBA2. Building TAPBA2 is a 12-story building, which is located near free-field station TAP022 (Figure 10). The recorded acceleration time histories may be used to identify the structural properties and to understand the structural responses during earthquakes. Comparing the responses at the basement and the roof of TAPBA2, the horizontal PGA in the roof was increased more than 3.5 times of the horizontal PGA in the basement. The fundamental frequency of building TAPBA2 is about 0.65 Hz to 0.7 Hz from the Fourier amplitude spectra constructed for the roof (Figure 12b) and is close to the dominant frequency shown in acceleration response spectra at station TAP022 (Figure 8).

Strong motion data collected from viaducts in Taipei City were also analyzed, as shown in Figures 13 and 15. Figure 13b shows the recorded acceleration response at the center span of a viaduct (Cheng-Kuo South Expressway). The maximum acceleration at the center of the span is 482 cm/sec^2 in the vertical direction. The dominant period of that signal is 1.57 seconds. Damage of bearing in this highway viaduct was observed during this earthquake. A permanent horizontal displacement about 3 cm in the bearing had been observed, as shown in Figure 14.

Acceleration response of another expressway viaduct (TAPBAB in Figure 10) was shown in Figures 15a–d. The recorded horizontal acceleration at the base was 60 cm/sec^2 ; and that at the top deck of the viaduct was 494 cm/sec^2 (the accelerometer at the top deck was located near the expansion joint where minor impact phenomenon

Table 3. Ground motion parameters recorded at selected stations

Station ID	Epicentral Distance (km)	PGA (cm/sec ²)	PGV (cm/sec ²)	$S_a(T=0.3)$ (cm/sec ²)	$S_a(T=1.0)$ (cm/sec ²)
HWA045	44.3	115.1	11.2	349.7	186.0
ILA050	48.3	260.6	12.5	514.7	58.1
ILA	72.2	120.3	19.2	248.5	225.0
TAP085	90.7	38.9	7.3	89.5	73.6
TAP082	94.0	15.3	3.1	36.0	23.0
TAP035	99.3	79.5	7.1	305.1	92.7
TAP053	104.0	83.8	8.4	310.7	89.0
TAP089	106.9	55.2	10.2	130.0	90.1
TAP109	107.6	115.9	21.6	196.0	297.8
TAP022	107.7	175.2	32.6	361.8	499.2
TAP015	108.5	102.2	22.4	170.7	271.0
TAP100	109.8	114.7	24.6	187.0	231.4
TAP032	109.8	156.8	25.7	313.7	274.3
TAP020	109.9	112.5	27.1	149.3	275.8
TAP	110.2	80.6	16.6	129.8	150.5
TAP013	111.6	84.1	21.0	163.4	231.9
TAP093	112.3	113.7	20.2	163.9	401.2
TAP043	113.4	79.1	13.0	157.2	225.3
TAP007	114.3	79.1	16.8	147.2	199.3
TAP017	116.0	65.3	22.0	103.5	171.4
TAP016	118.4	57.4	17.6	92.3	119.8
TAP004	119.1	54.8	16.8	69.9	124.1

was observed). The amplification on peak acceleration was significant. Wavelet analysis was used to study the response data. Figure 15d shows the amplitude-frequency-time spectrum of the recorded bridge response at the deck of the viaduct. From Figure 15d it is found that high-frequency signals (10~12 Hz) exist in the response data. Detailed study is required on the high-frequency signal in the response data with respect to damage feature.

BUILDING DAMAGE INVESTIGATION

Because of the basin effect this earthquake caused major damage in Taipei City and Taipei County. (The population in Taipei City is about 2.6 million in an area of about 270 square kilometers, while the population in Taipei County is about 3.5 million in an area of about 2,000 square kilometers.) In the first-stage evaluation after the earthquake, 6 buildings in Taipei City and 40 buildings in Taipei County were posted with red tags (denoting danger and that entrance to the building is restricted), and 62 buildings in Taipei City and 254 buildings in Taipei County were posted with yellow tags (denoting that entrance to the building should be cautious). Building reconnaissance includes commercial/residential buildings and school buildings. The building damage modes for

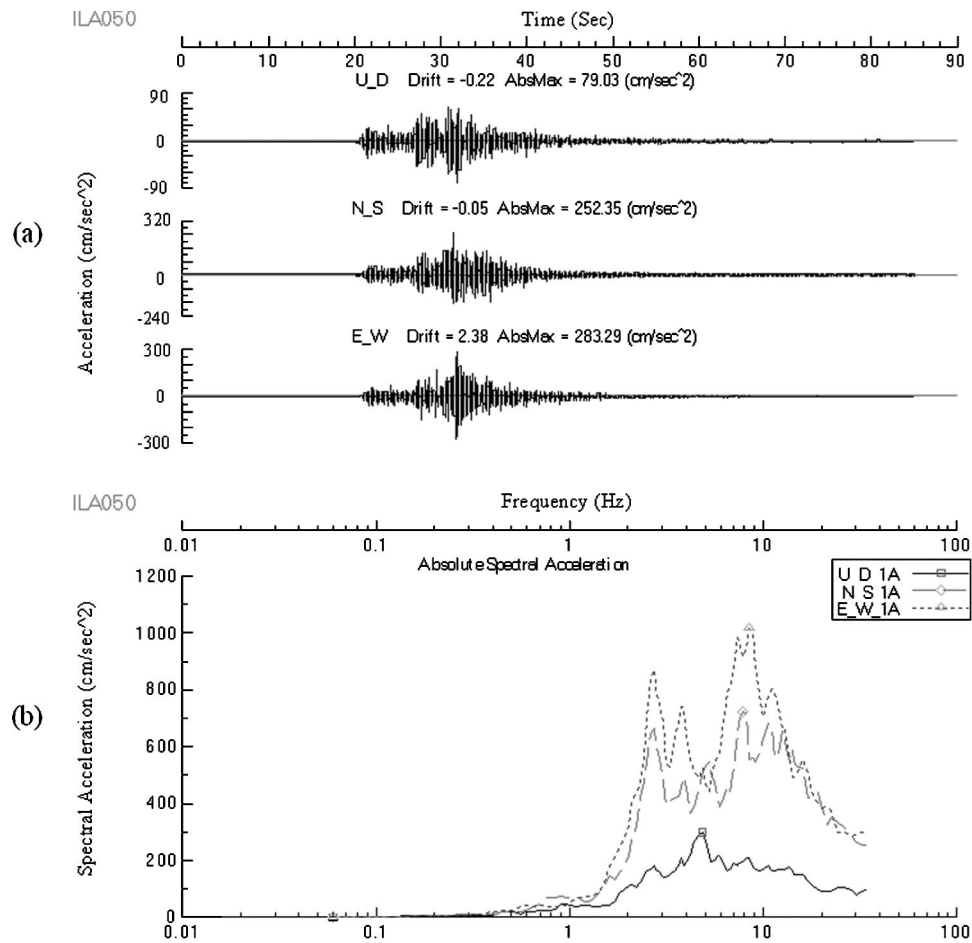


Figure 5. (a) The recorded acceleration time histories, and (b) the calculated acceleration response spectra (5% damping) of station ILA050, which had the largest PGA and the largest acceleration response spectra in the 31 March 2002 earthquake.

the 31 March earthquake can be summarized as follows: (1) presence of soft and weak first story, (2) lack of redundancy, (3) lack of lateral reinforcement, and (4) imbedded pipelines in column.

DAMAGE INVESTIGATION OF COMMERCIAL/RESIDENTIAL BUILDINGS

In urban and township areas, the most common building structure is the mixed commercial and residential building designed with a corridor to provide pedestrian walkway. Low-rise buildings, of three to five stories high and composed of several units, are often lined up in a row along the street. This type of building was constructed in early 1970s. The plan of each unit is about 4.5 m wide along the corridor and 12.5 m deep perpendicular to the corridor (Figure 16). The brick walls are first erected, and reinforced con-

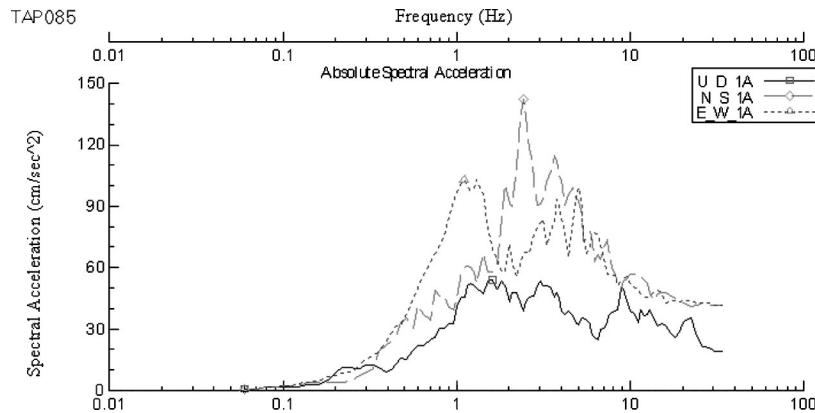


Figure 6. The calculated acceleration response spectra (5% damping) of station TAP085. The intensity was reduced due to attenuation.

crete columns, beam and slab are then constructed by using the brick walls as part of the formwork. They are classified as reinforced-masonry buildings in Taiwan. Perpendicular to the corridor, two adjacent apartment units are partitioned with a common brick wall that is continuous in the gravity direction. However, along the corridor, there are doors and windows for entrance and natural light, and no walls are continuous in the gravity direction. Damage was observed in this type of building. Figure 16 shows the plan view of the building as well as the damage feature. Columns along corridors were seriously damaged and subsequently shored with steel columns and jacks. Similar damage features were also observed in a 5-story condominium building, as shown in Figure 17.

In addition to the provision of corridors, large openings for doors and windows are necessary at the street side of the buildings. Moreover, if the developers, builders, or owners provide open space for the public at the ground level, they are allowed to build more floor areas as a reward. On the other hand, the frames above the ground floor are in-filled with a brick masonry perimeter and partition walls. Thus, the bottom floor is comparatively soft and weak due to the presence of corridors, the open front, and open space. This is the case of soft first-story damage mode. The only collapsed building during the earthquake was one of the soft first-story buildings. The schematic elevation and plan views of the collapsed 5-story mixed commercial and residential building are shown in Figure 18. The basement and the first floor of the building are for commercial use and the rest of the floors are for residential use. The building was constructed between 1974 and 1975. There are a total of 12 columns. Along the long axis, a corridor is provided and the number of spans ranges from three to four. But the number of spans along the short axis just ranges from one to two spans, so that redundancy is highly inadequate. In this earthquake, the first and second floor collapsed and tilted 5 degrees toward the street side (Figure 18c).

The most detrimental construction is found in all pipelines, including water supply, drainage, and electricity imbedded inside the columns, particularly in the exterior col-

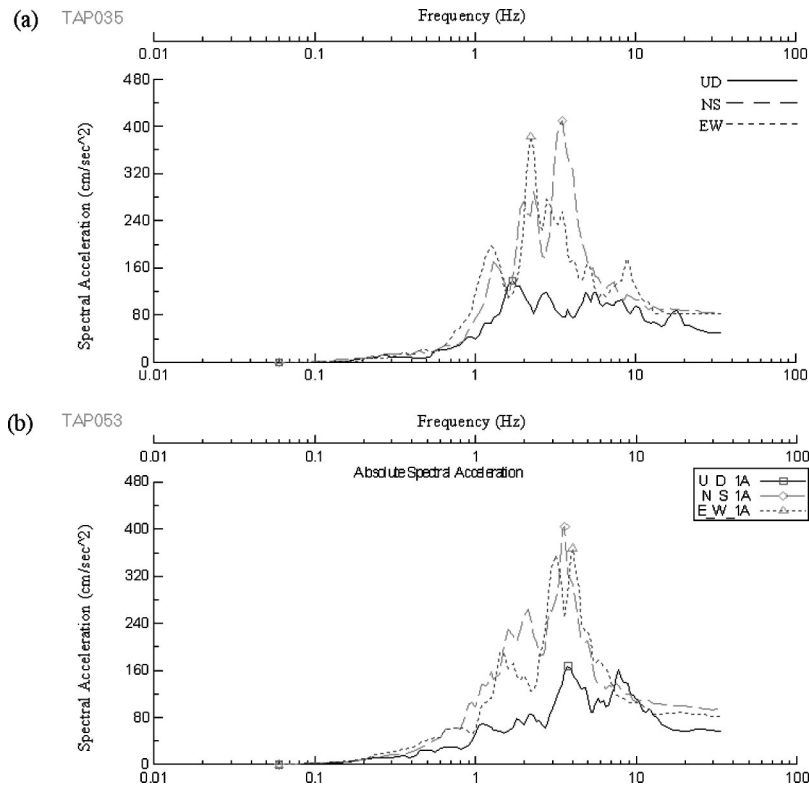


Figure 7. The calculated acceleration response spectra at (a) TAP035 and (b) TAP053. Being located at the peripheral region of Taipei Basin, the spectral intensity around 2 to 4 Hz starts to increase significantly.

umns, as shown in Figure 19. Consequently, the effective area of the reinforced concrete columns is greatly reduced. The area of the columns may not be very large. After a drainage pipe that is usually more than 5 cm in diameter is imbedded, the area occupied by the pipe cannot be neglected and the reinforcement becomes more congested. In the damaged column the space of lateral reinforcement in the columns of existing buildings may exceed 20 cm. The ties usually have 90-degree hooks with no cross ties. Since lateral reinforcement is very useful in providing confinement for core concrete, prolonging buckling of longitudinal reinforcement and prohibiting shear failure, the strength of the column is reduced due to the imbedded pipes. Besides, the defective structural system is an important cause of building damage. For example, it is common practice to lap-splice the longitudinal reinforcement at the same location just above the ground floor. Relative slippage of longitudinal reinforced bars may occur with the lack of lap length and lateral reinforcement. Thus there is a tendency that the columns of such buildings are in the mode of brittle failure. Since the population is dense and the basement is not considered as floor area, deep excavation is very common for mid- to high-rise buildings. The basement is usually used for parking cars. In order to maximize the number of cars to be

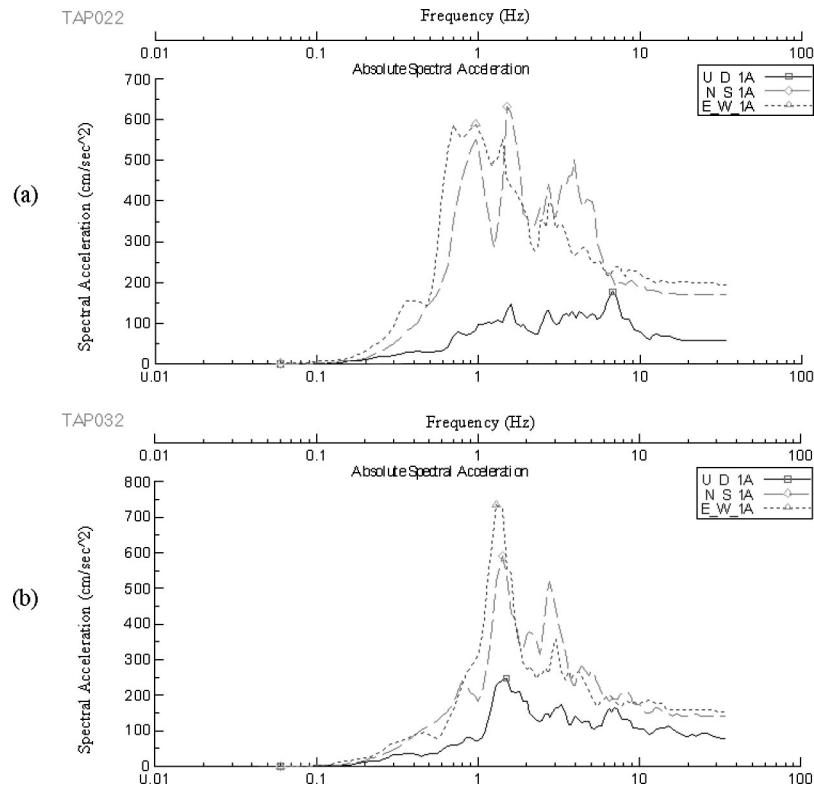


Figure 8. The calculated acceleration response spectra at (a) TAP022 and (b) TAP032. The low-frequency energy around 0.7 to 2 Hz was amplified significantly due to basin effect.

parked and to provide enough space for the mobility of the cars, the number of columns is minimized and the span between columns is maximized. Due to lack of redundancy, once one of the columns is damaged, the rest of columns will be damaged sequentially.

DAMAGE INVESTIGATION OF SCHOOL BUILDINGS

Besides the damage to commercial/residential buildings in the Taipei metropolitan area, damage to school buildings is also significant. In Taiwan, most school buildings at the primary and secondary level lack integral planning. If the budget allows, new school buildings will be built in the horizontal or vertical directions of the existing school buildings at different times in order to solve the problems of insufficient classrooms. Due to the lack of adequate planning, the original structural system is seriously undermined. Most school buildings were constructed and expanded in a patchy way, and this caused insufficient seismic resistance as an aftermath. The new school buildings expanded in the horizontal direction are usually connected with old school buildings to provide some continuity of activity space for pupils and teachers. Being constructed at different times, the old school buildings and the new school buildings may possess dif-

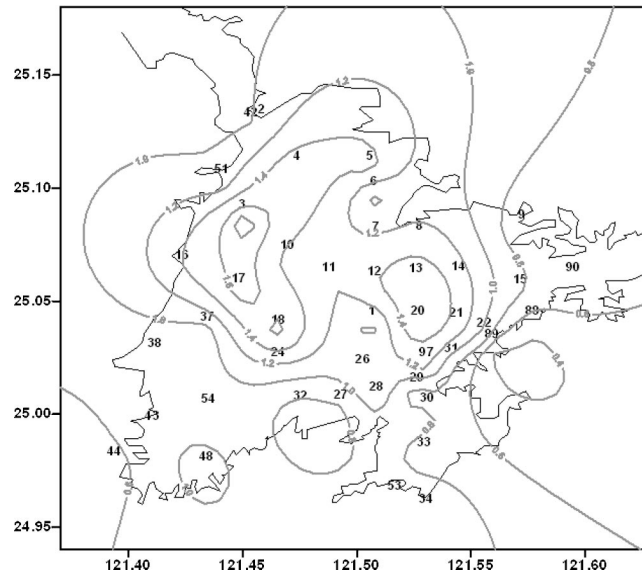


Figure 9. Contour map of dominant period (in seconds) of Taipei Basin. The identified basin dominant period was estimated from ground motion data collected from the Taiwan Strong Motion Instrumentation Program of the Central Weather Bureau (from Loh et al. 1998).

ferent fundamental vibration periods. Therefore, when an earthquake strikes, the old and new school buildings do not vibrate in-phase. Pounding between two adjacent school buildings due to insufficient seismic gap can often be observed.

The structural systems of school buildings have intrinsic defects. Classrooms are



Figure 10. Distribution of structural array systems and free-field stations, installed by the Central Weather Bureau, in the Taipei area. The house symbols indicate the structural array systems and the circular symbols indicate free-field stations. Structural responses of TAPBA2, TAPBA8, and TAPBAB were demonstrated in this paper.

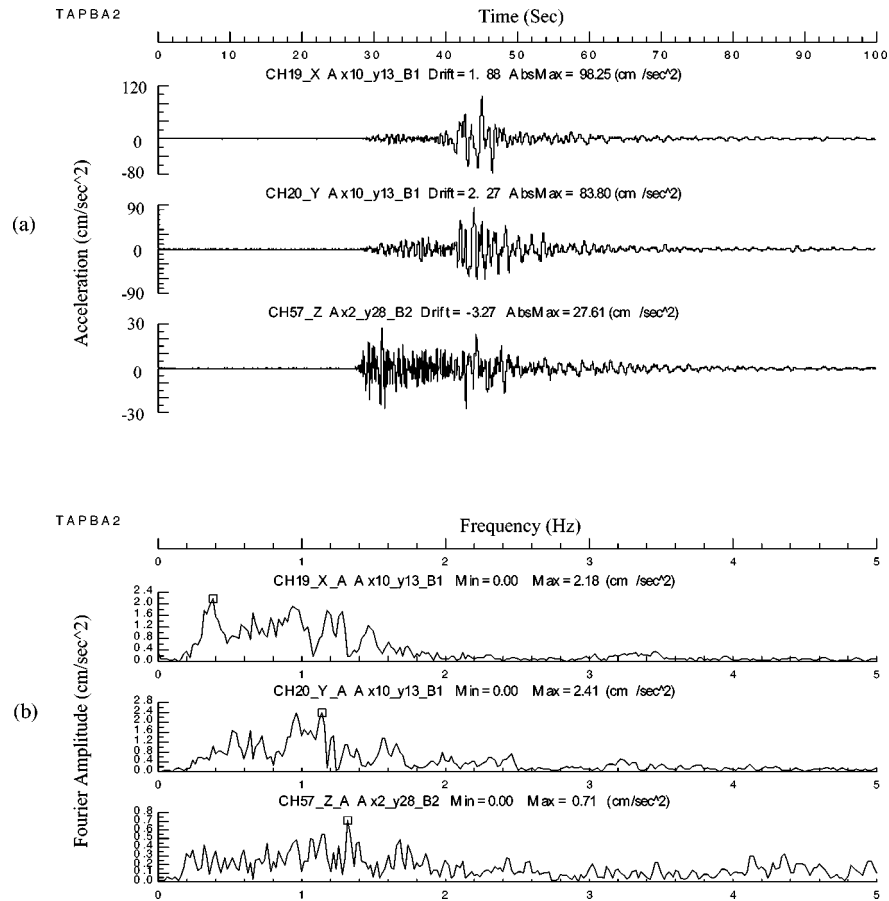


Figure 11. (a) The acceleration time histories, and (b) the Fourier amplitude spectra in three directions at the basement of building TAPBA2. X, Y, and Z directions correspond to two horizontal major axes and up-down direction, respectively.

generally located side by side in a row. The plan of each classroom is about 10 m in width along the corridor and 8 m in depth perpendicular to the corridor. There may be just one corridor in front of the classrooms or one at each side of the classrooms. The corridor may or may not be cantilevered. Figure 20 shows the schematic elevation and plan views of a typical 2-story school building. The stiffness in direction perpendicular to the corridor is much higher than that along the corridor, and there is a strong tendency for damage to occur in this type of situation. In order to utilize the natural light and ventilation, windows and doors fully occupy both sides of the corridor. At the upper portion of the columns, the columns are constrained by the window frame made of aluminum. At the lower portion of the columns, they are constrained by the windowsill made of brick walls. Since the windowsill is rigid compared with the window frame, the effective length of the column is shortened. The shorter the column, the larger the shear force. Therefore, the columns tend to fail in the shear mode rather than in the flexural

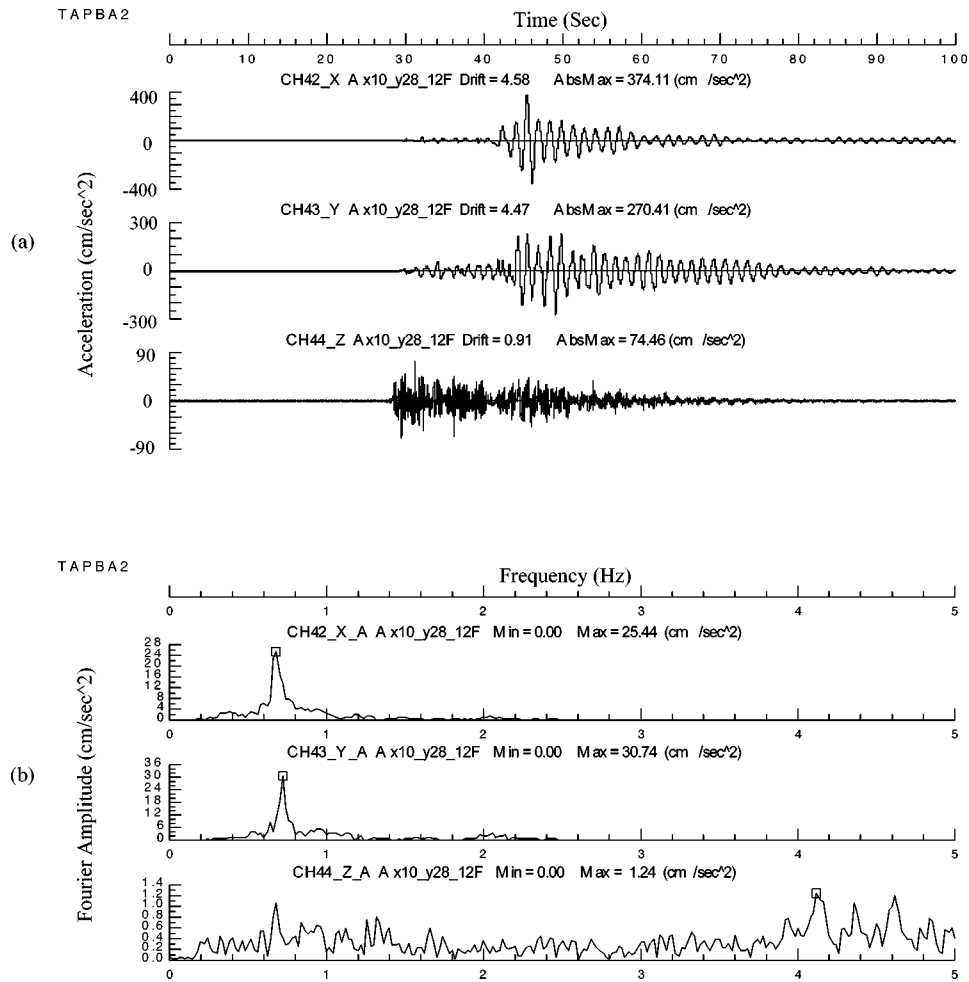


Figure 12. (a) The acceleration time histories, and (b) the Fourier amplitude spectra in three directions at the roof (12th floor) of building TAPBA2. X, Y, and Z directions correspond to two horizontal major axes and up-down direction, respectively.

mode. Figures 21a and 21b show that the columns were damaged along the direction of the corridor. Short columns were revealed by the diagonal shear cracks.

When the corridors are cantilevered, there is only one span in the direction perpendicular to the corridor, and the redundancy for such structural system is highly inadequate. Without sufficient redundancy, stress cannot be redistributed effectively and the ductility of the structures is not satisfied.

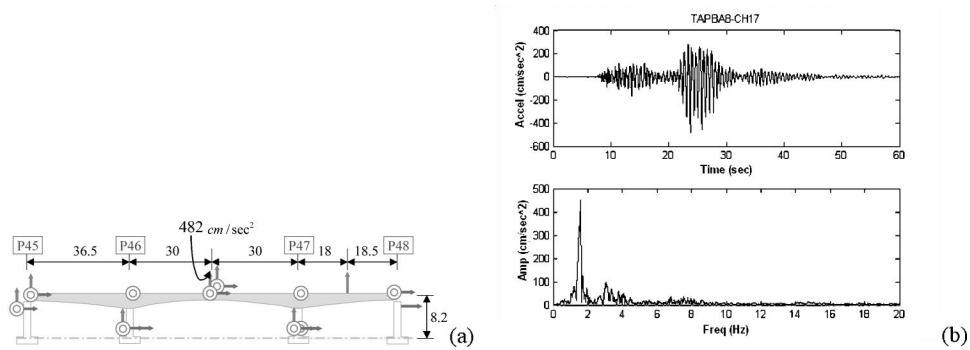


Figure 13. (a) Side view of and instrumentation layout at the Chang-Kuo Viaduct (TAPBA8) in Taipei City. The recorded peak acceleration at mid-span of the viaduct in vertical direction is 482 cm/sec², and (b) recorded acceleration time history and the corresponding Fourier amplitude spectrum (in vertical direction) at the mid-span of the viaduct.

OBSERVED DAMAGE IN THE TAIPEI FINANCIAL CENTER CONSTRUCTION SITE

The Taipei Financial Center (TFC), planned to be the tallest building in the world, will reach a height of 508 meters when it is completed. Four tower cranes have been installed to erect the steel works of the building tower. On 31 March 2002, the construction of the TFC had reached the point of erecting the steel frame members for the 53rd up to the 56th floors of the building. During the main shock of the earthquake that day,



Figure 14. Damage of bearing of the Chang-Kuo Viaduct in Taipei City. A 3-cm permanent displacement was observed on the bearing.

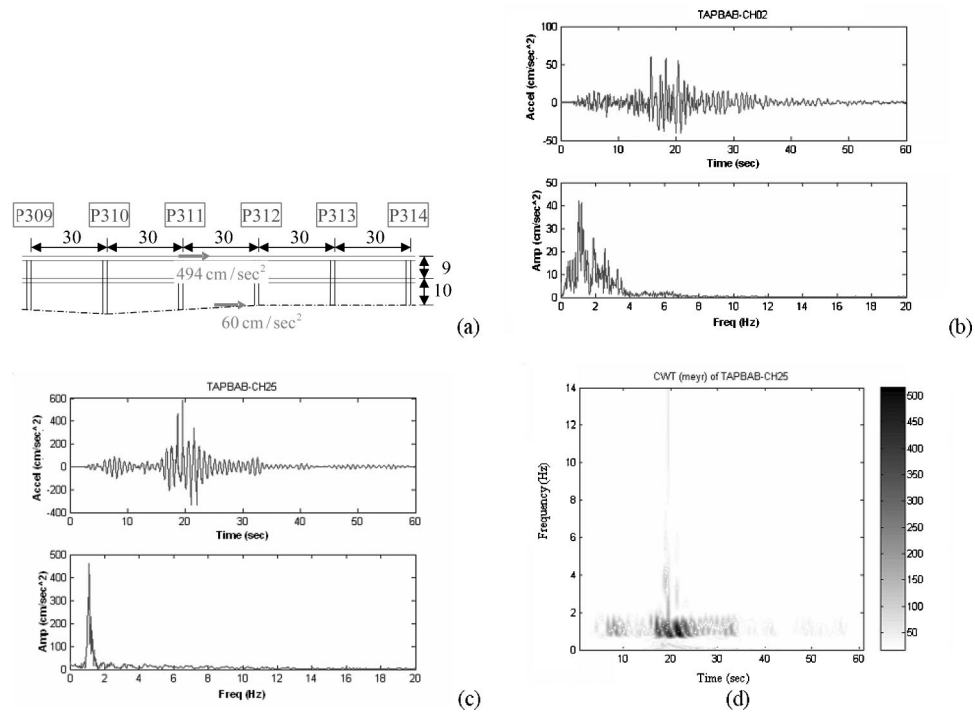


Figure 15. (a) Side view of and the recorded maximum acceleration of TAPBAB, which is one of the viaducts in Taipei City; (b) and (c) recorded acceleration time histories and the corresponding Fourier amplitude spectra at the ground and the top deck of the viaduct shown in part (a); and (d) continuous wavelet analysis from data collected at the top deck of the viaduct.

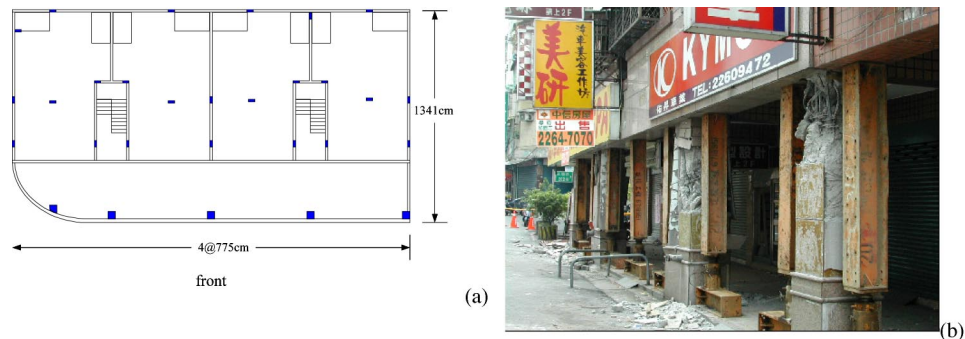


Figure 16. (a) Schematic plan of a 5-story condominium building, and (b) columns along corridor that were seriously damaged and shored with steel columns and jacks.

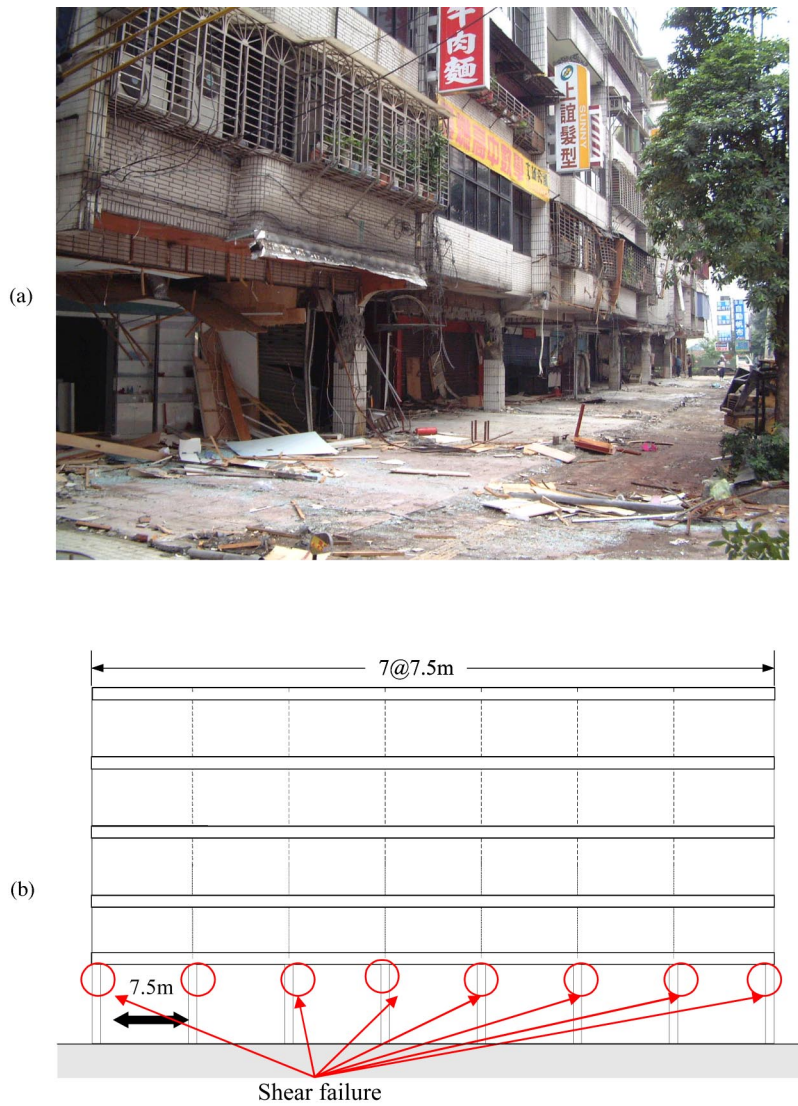


Figure 17. (a) Photo of a damaged 5-story building with seven units in a row, and (b) schematic diagram of the building in (a) and the damage locations of the columns along the corridor.

among four tower cranes, two collapsed and one was severely damaged with crane counterweights falling off one end of the boom, as shown in Figure 22. The incident killed two corresponding crane operators, two steel workers near the 53rd floor and one part-time student worker on the ground. This article reports on the damages of the TFC structure observed following the 31 March earthquake and discusses the ground accelerations recorded at two nearby free-field strong-motion stations.

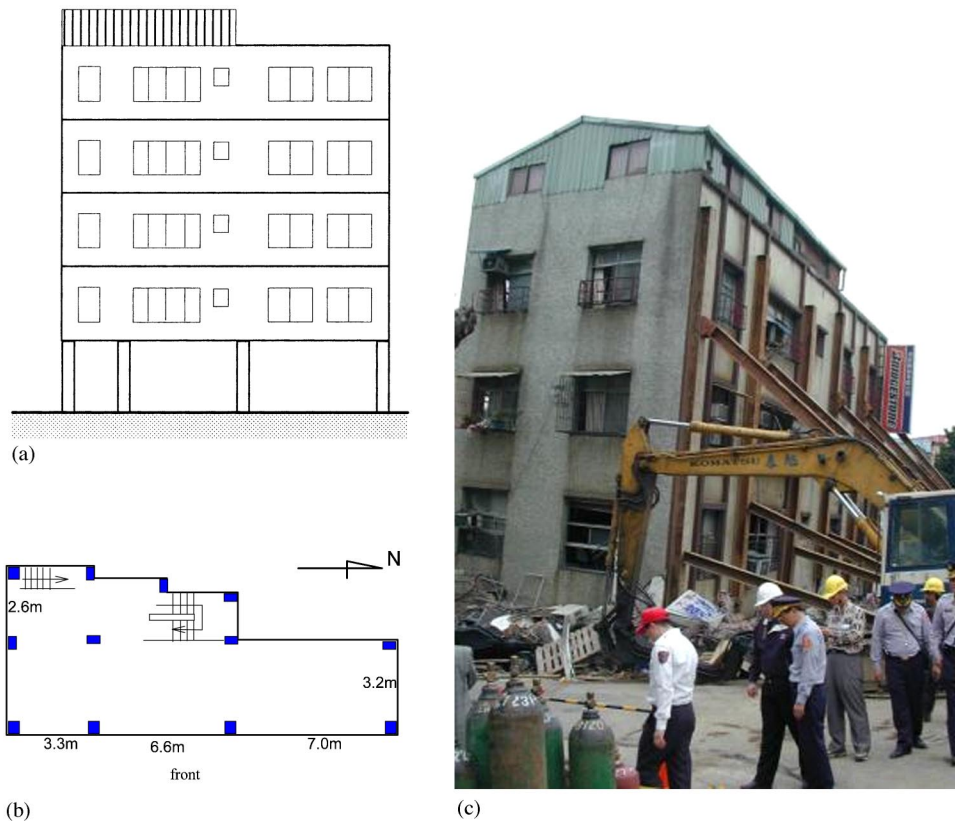


Figure 18. Schematic elevation (a) and plan (b) views of a 5-story apartment building. The 5-story building collapsed (c) in the 31 March earthquake due to a soft first story and poor configuration of the structural system.

STRUCTURAL DESIGN AND CONSTRUCTION OF TFC

When completed, TFC will consist of a 101-story office tower and a podium to be used as a shopping mall. The structures for the office tower and the podium are completely separated by the expansion joints, but the 5-story basement of the entire TFC is interconnected. The floor plan of the TFC tower is shown in Figure 23. The typical composite-floor framing system is made by using concrete topping over the metal deck and the welded shear studs on the steel beams. The TFC tower lateral force-resisting system primarily consists of a steel-braced central core frame interconnected to eight perimeter mega columns by outrigger trusses every eight floors (Shieh and Chong 2001). Most of the beam-to-column connections are moment connections. The mega and other box columns in the TFC tower are in-filled with high-strength concrete (10,000 psi or 70 Mpa compressive strength). The floor framing system for the podium is the same as that in the tower, but the lateral force-resisting system is a welded steel moment-frame. The foundation of the TFC tower consists of pile caps on top of 1.5-meter-diameter and

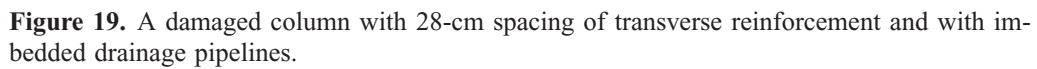


Figure 20. Schematic side elevation view (a), and plan view (b), of a school building.

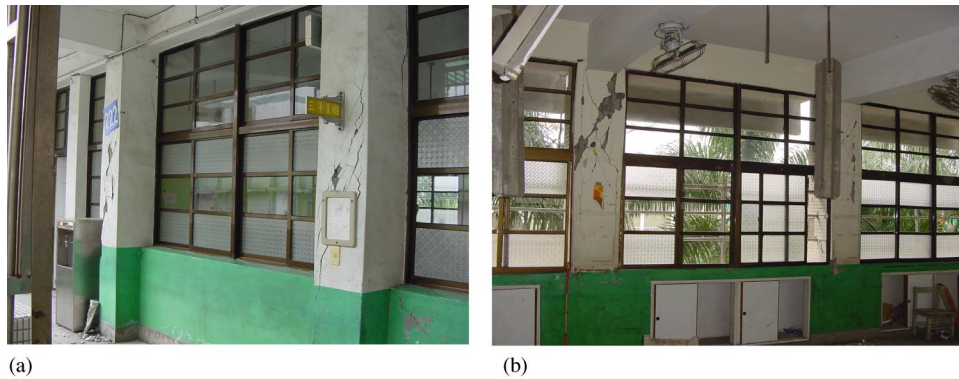


Figure 21. (a) Columns were damaged along the direction of the corridor; and (b) diagonal shear cracks were due to the short column effect, and the lighting facility had fallen down.

TOWER CRANES FOR THE CONSTRUCTION OF TFC TOWER

A total of four tower cranes (TC#1 through TC#4), as shown in Figure 24, had reached a height of about 260 meters on 31 March 2002 for lifting the material or equipment for the construction of 53rd to 56th floors. These four cranes were designed based on the New Zealand Seismic Standards. The tower cranes TC#1 and TC#3, located near

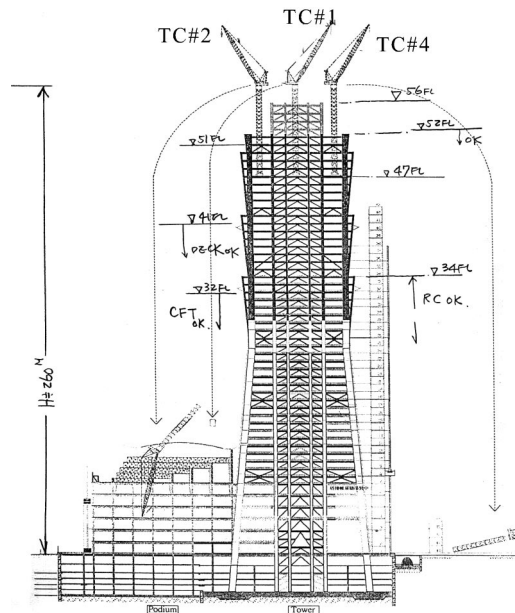


Figure 22. Elevation view of the frame and tower cranes of TFC construction site. The locations of two fallen cranes are also indicated in this figure.

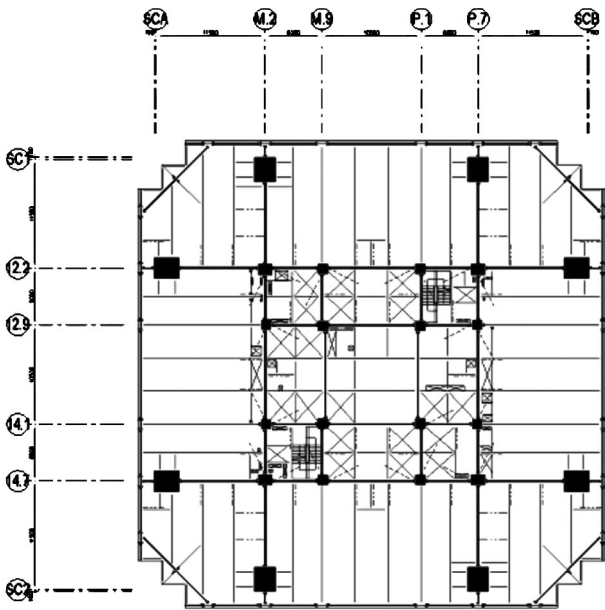


Figure 23. Plan view of the frame system on the 47th floor of the TFC construction site.

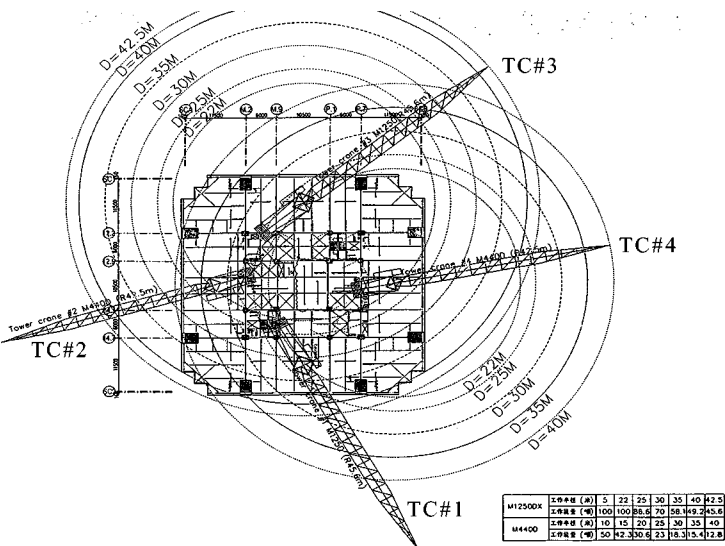


Figure 24. Plan view of the locations of the four tower cranes at the TFC construction site.

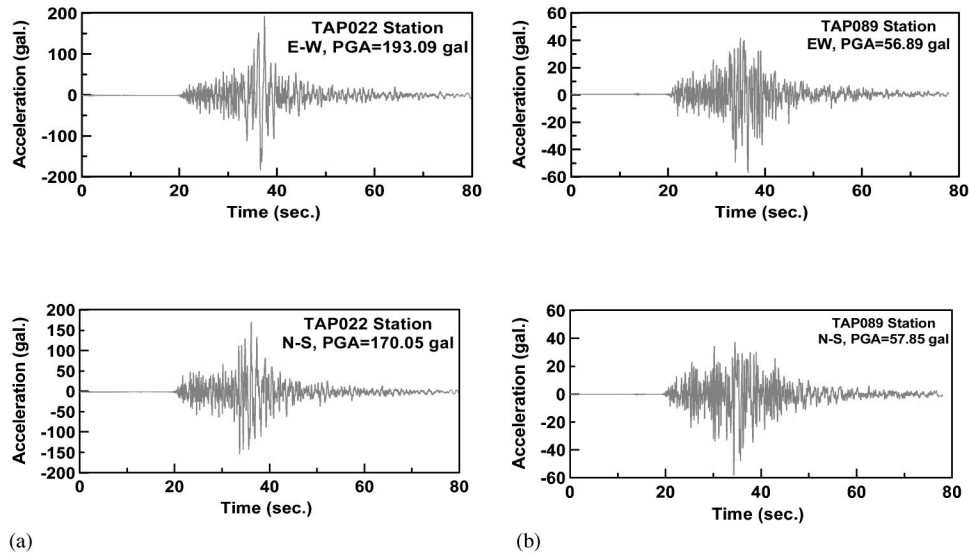


Figure 25. Acceleration time histories of stations (a) TAP022, and (b) TAP089.

the southern and northern sides of the TFC building, respectively, are identical (Model M1250D with a lifting capacity of 22,000 kN-m). TC#2 and TC#4 were also identical (Model M440D), with a lifting capacity of 6,500 kN-m. The New Zealand Seismic Standards require that the tower crane must remain functional after an earthquake of $\text{PGA}=0.088\text{ g}$ occurred when the tower crane is fixed on the ground but not in operation. The four tower cranes also meet the seismic lateral force requirements (a shear force of 20% self-weight) stipulated in the JIS and Taiwanese construction safety standards. In order to laterally support the tower crane as it goes up to specific floors, the steel fabri-

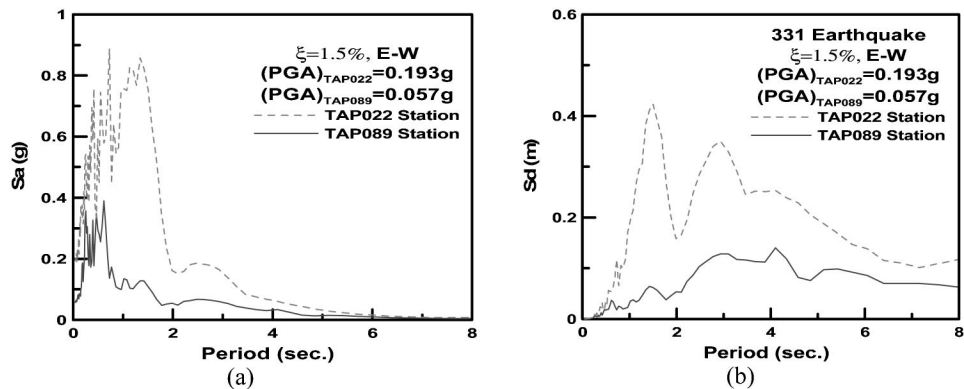


Figure 26. Acceleration (a), and the displacement (b) response spectra, with 1.5% damping at stations TAP022 and TAP089, in the 31 March earthquake.



Figure 27. (a) Collapse of TC#2 at 51st floor, and (b) collapse of TC#4 above the 51st floor.

cator has further considered both the wind loads and the dynamic horizontal shear responses, at the tower crane anchoring levels, resulted from a design earthquake of $PGA = 0.1 \text{ g}$ (10% chance of exceeding in 3 years) occurred on the ground (Tsai et al. 2002a, CEER 2002).

GROUND ACCELERATIONS RECORDED IN THE NEARBY FREE-FIELD STRONG-MOTION STATIONS

The site of the TFC building is located at the southeast side of Taipei Basin where a deep alluvium deposit has been identified. Ground accelerations recorded in the main shock of the 31 March earthquake in the TAP022 and TAP089 stations may be useful in assessing the seismic demand imposed on the structures in the region. As shown in Figure 10, the TAP089 site is about 2 km toward the southeast of the TFC and near the foothill of Taipei Basin, while TAP022 is only about 300 m south of the TFC. The variations of ground motion intensity are evident (Figures 25a and 25b) as the PGA in the east-west direction is 0.193 g in station TAP022 and only 0.057 g in TAP089. The elastic acceleration response spectra are given in Figure 26 for a damping ratio of 1.5%. It should be noted that it is estimated from detailed analysis that the fundamental periods of the four tower cranes are about the same as 2.2 and 2.7 seconds for TC#1 and TC#2, respectively, while that of the superstructure of the TFC at the time of the incident is about 2.2 seconds (Tsai et al. 2002a).

DAMAGE AT THE CONSTRUCTION SITE OF TFC TOWER

When the main shock of the 31 March earthquake struck the TFC building construction site, the crane operators of TC#2 and TC#4 were in the control rooms but the cranes were not in operation. TC#1 was erecting one of the perimeter sloping columns for the 53rd up to the 56th floors near the building's southwest corner. During the shaking, apparently, the mast of both TC#2 and TC#4 fractured near the 51st floor and collapsed, as shown in Figure 27. The collapsing boom of TC#4 hit and broke the cable of TC#1. Consequently, the shaking not only resulted in the falling of TC#2 and TC#4, but also caused

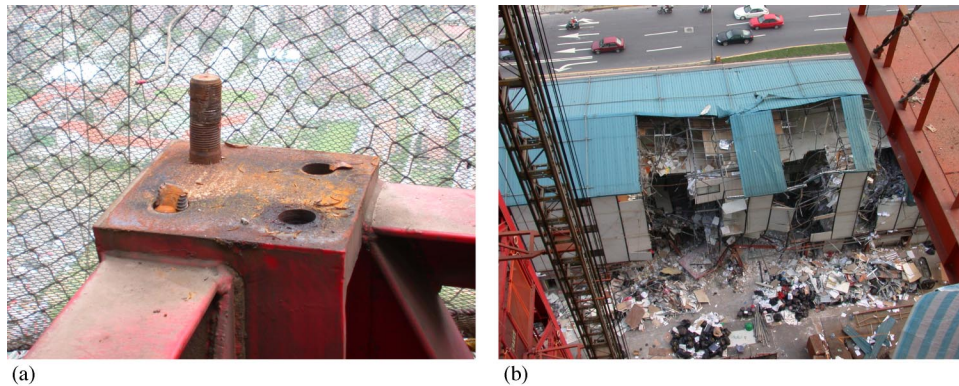


Figure 28. (a) Failure at the bolted column splice, and (b) damage at the construction site office caused by the falling counterweights.

the falling of the column being erected by TC#1. In addition, the strong shaking together with the sudden release of the lifted column weight seem to be responsible for all the counterweights (15 pieces, 75 kN each) of TC#1 falling from the rack and dropping from a height of about 260 m (Figure 22). Some of these counterweights hit the ground and caused substantial damage to construction equipment and material. Two pieces of the counterweights hit and damaged a significant part of the construction site office (Figure 28b). Some of the falling counterweights penetrated the metal deck, severely damaging several steel beam members before stopping at the 34th concrete floor slab. The falling boom of TC#2 hit and penetrated the roof structure of the podium, and the collapsed TC#4 landed on the adjacent street. Due to the severe vibrations and the impacts caused by the falling counterweights, various construction material and equipment, including some welding machines, high-tension bolt containers, and damaged steel members fell from high floors. Some of the falling pieces knocked off some edges of the concrete slab and damaged the perimeter curtain walls near the lower floors before landing on the ground.

Immediately following the incident at the TFC construction site, the city government closed the streets surrounding the building site to all automobile and pedestrian traffic. This incident injured many people, including some workers and pedestrians, and killed the crane operators in TC#2 and TC#4, two steel workers, and one part-time worker on the ground floor near the construction site office. Tower Crane TC#3 appears to have survived the 31 March earthquake after the inspection, and the trial lifting started about ten days following the main shock. However, TC#3 is not capable of removing the already damaged TC#1 for repair; therefore, a rescue Tower Crane TC#A has been proposed to replace TC#4, to help remove the collapsed TC#2 and to repair crane TC#1.

CAUSE OF INCIDENT

The incident that occurred at the TFC construction site made world headlines immediately following the 31 March Taiwan earthquake. Results of site investigations (Weng

et al. 2002) indicate that both TC#2 and TC#4 failed at the column splices where four 45-mm-diameter high-strength bolts were used at each splice (Figure 28a). Preliminary test results show that the typical failure mode of the high-tension bolt is the shearing-off of the threads, but not the tensile fracture of the bolt cross section. Test results (CEER 2002, Tsai et al. 2002a) also confirm that the shear-off failure load of the bolts is about 1250 kN. Three-dimensional analytical results (Tsai et al. 2002b, 2003) of simplified TFC building stick models incorporating the four tower cranes suggest that the peak horizontal acceleration at the 51st floor is as high as 0.8 g under the effects of simultaneous applying the two horizontal components of the TAP022 recorded accelerations. The elastic demand-to-capacity ratios of the tower crane column splices considering a tensile capacity of 5000 kN at each splice are in the range of 2.0 to 3.0. The high seismic demands imposed on the tower crane bolted splices due to a strong earthquake, significantly greater than the tower crane was designed for, appear to be the key factors responsible for the collapse of the tower crane. At the time of this writing, a stiffened and strengthened scheme has been proposed by the general contractor for the rescue Tower Crane TC#A to be used in the restoration work of the TFC construction project.

CONCLUSIONS

This paper presents a general overview of the earthquake disaster that occurred in Taiwan on 31 March 2002. Although the epicenter of the earthquake is located offshore of the northeast side of Taiwan, the damage was concentrated at Taipei City and its surrounding area. From the strong motion data collected by the Central Weather Bureau, the maximum PGA at Taipei City is about 200 cm/sec². Significant variation of free-field ground motion across the basin was observed due to basin effect. Building reconnaissance included commercial/residential buildings and school buildings.

ACKNOWLEDGMENTS

The authors wish to express their appreciation to the Central Weather Bureau for providing seismic response data of free-field and structures for this study. Data processing by Mr. S. K. Huang (research assistant at NCREC) is acknowledged. The general contractor, the design engineers at the Evergreen Engineering Consultants, and the Tsai Tong-Ho Structural Engineering Consultants for providing information on the damage of TFC are also acknowledged.

REFERENCES

- Jean, W. Y., 2001. A study on the characteristic earthquake and site effects and its application to the hazard evaluation, Report of National Center for Research on Earthquake Engineering, Taiwan, *NCREC-01-036*.
- Loh, C. H. and Yeh, C. H., 1998. Researches related to seismic hazard mitigation in Taiwan, *J. of the Earthquake Engineering Society of Korea* **2** (3), 13–26.
- Loh, C. H. and Tsay, C. Y., 2001. Responses of the earthquake engineering community to the Chi-Chi (Taiwan) earthquake, *Earthquake Spectra* **17** (4), 635–656.
- Loh, C. H., Hwang, J. Y., and Shin, T.-C., 1998. Observed variation of earthquake motion across a basin-Taipei City, *Earthquake Spectra* **14** (1), 115–133.
- Review Meeting Records, 2002. Review of the restoring plan for the Taipei Financial Center

- building after the 331 Earthquake, Center for Earthquake Engineering Research, College of Engineering, National Taiwan University, April 13 and 22.
- Shieh, S. S. and Chong, C. H., 2001. The design and construction of the Taipei Financial Center, *Proceedings of the Second Taiwan-China-Hong Kong Tri-lateral Conference on Technology of Steel Structures*, November 2001, Taipei.
- Tsai, K. C., Shieh, S. S., Tsai, T. H., Shirai, T., Chong, C. H., Chang, J. C., Lin, P. Y., and Weng, Y. T., 2002a. Personal communications from 6th to 12th of April.
- Tsai, K. C., Weng, Y. T., and Shieh, S. S., 2002b. Response analysis of tower cranes collapsed during the 331 Taiwan Earthquake, *Structural Engineering* **17** (3), Chinese Society of Structural Engineering (in Chinese).
- Tsai, K. C., Weng, Y. T., Yeh, C. H., and Shieh, S. S., 2003. Earthquake collapse of the tower cranes in the construction of the 101-story tall building in Taiwan, *Proceedings, Response of Structures to Extreme Loading*, Toronto, August.
- Weng, Y. T., Tsai, K. C., and Shieh, S. S., 2002. Observed damages of Taipei Financial Center construction, *Proceedings of Workshop on the Results of the 331 Earthquake Damage Reconnaissance*, National Center for Research on Earthquake Engineering, April 19, 2002 (in Chinese).

(Received 20 May 2002; accepted 7 April 2003)